

# Scaling of the dynamical properties of the Fermi-Ulam accelerator model

Denis Gouvêa Ladeira<sup>1,\*</sup> and Jafferson Kamphorst Leal da Silva<sup>1,†</sup>

<sup>1</sup> *Departamento de Física, ICEx  
Universidade Federal de Minas Gerais  
Caixa Postal 702, 30.123-970,  
Belo Horizonte/MG, Brazil*

(Dated: September 19, 2018)

The chaotic sea below the lowest energy spanning curve of the complete Fermi-Ulam model (FUM) is numerically investigated when the amplitude of oscillation  $\varepsilon$  of the moving wall is small. We use scaling analysis near the integrable to non-integrable transition to describe the average energy as function of time  $t$  and as function of iteration (or collision) number  $n$ . If  $t$  is employed as independent variable, the exponents related to the energy scaling properties of the FUM are different from the ones of a well known simplification of this model (SFUM). However, if  $n$  is employed as independent variable, the exponents are the same for both FUM and SFUM. In the collision number analysis, we present analytical arguments supporting that the exponents  $c^*$  and  $b^*$  related to the initial velocity and to  $\varepsilon$  are given by  $c^* = -1/2$  and  $b^* = -1$ . We derive also a relation connecting the scaling exponents related to the variables time and collision number. Moreover, we show that, differently from the SFUM, the average energy in the FUM *saturates* for long times and we justify the physical origins for some differences and similarities observed between the FUM and its simplification.

PACS numbers: 05.45.-a, 05.45.Pq

Keywords: Fermi model, chaos, scaling

## I. INTRODUCTION

The Fermi accelerator is a dynamical system, proposed by Enrico Fermi [1] to describe cosmic ray acceleration, in which a charged particle collides with a time dependent magnetic field. With base in different applications, the original model was later modified and studied by other authors. One of them is the well known Fermi-Ulam model (FUM) [2, 3], in which a ball is confined between a rigid fixed wall and an oscillatory moving one. In this model the ball collides elastically with the walls and the system is described by an area preserving map. In high energies regime the phase space presents Kolmogorov-Arnold-Moser (KAM) islands surrounded by locally chaotic regions, which are limited by spanning curves. Below the invariant spanning curve of lower energy a globally chaotic sea involves KAM islands. The presence of invariant spanning curves limits the orbits in phase space impeding unlimited energy growth (Fermi acceleration) [3, 4]. Another model, very similar to FUM, in which the ball is in a gravitational field, so-called bouncer [5], presents, differently from FUM, the property of Fermi acceleration depending on values of control parameter and initial conditions. This difference between the two models was later explained by Lichtenberg et al [6]. Hybrid versions [7] involving both FUM and bouncer and versions of FUM with energy dissipation [8] were also explored. Quantum models based on FUM and bouncer have also been studied [9, 10, 11]. The study of such systems is interesting because it allows to compare theoretical predictions with experimental results [12, 13]; moreover the knowledge about how time-dependent perturbations affect the dynamics of Hamiltonian systems is something that needs to be more ex-

plored. Therefore it is useful to study such perturbations in simple models because they furnish insights about more complex systems; even more, the formalism used in its characterization can be extended to the billiard class of problems [14, 15, 16, 17].

The simplified Fermi-Ulam model (SFUM) [2] is an approximation in which the position of the *moving wall* is considered as *fixed*, but it transfers momentum and energy to the particle. This geometrical change of the complete model can be neglected when the amplitude of oscillation is much smaller than the distance between the two walls and the velocity of the particle is larger than the wall maximal velocity. It is clear that the simplified versions can speed up the simulations. However the main interest in these simplified models is that they can be studied by analytical methods whose results are often compared with the numerical results of the simplified model. Moreover, these analytical results are, sometimes, also useful in study of the full models.

The moving wall in the Fermi-Ulam model represents an external force that acts as a perturbation in the system. If the oscillation amplitude of the moving wall is zero the system is integrable but as soon as this amplitude is different from zero the Fermi-Ulam model behaves chaotically [18]. Near the integrable to non-integrable transition, average quantities can be described by scaling functions. This kind of analysis was originally proposed in a study of the SFUM, where the collision number with the moving wall is employed as independent variable [19]. In a recent work [20], also based on the SFUM, we proposed a similar analysis in which time is considered as independent variable and we showed that the average energy can also be described by scaling functions but with a different exponents set. Moreover, we showed that the

average energy *decays* at long times.

In the present work we investigate the chaotic sea below the spanning curve of lowest energy for the full Fermi-Ulam model, where scaling properties of average energies are studied on variables *time* and *iteration* (or *collision*) *number*. We show that if the time is employed as independent variable, then the exponents related to the scaling properties of FUM are not the same that the ones of SFUM. However, if the iteration number is employed as independent variable, then both FUM and SFUM present the same set of exponents. We show that the energy decay found for long time in the SFUM [20] does not exist for the FUM and we justify physically the origins of the similarities and differences between the FUM and SFUM. We provide also some analytical results for the scaling exponents and, moreover, we show that although the exponents related to the variables *time* and *collision number* are not the same a relation between them can be established.

This paper is organized as follows: In the next section the Fermi-Ulam model and the average quantities of interest are defined. We present also the procedures to obtain these averages when time is the independent variable. In Section III we present the results of the numerical simulations, the scaling properties of average energies as function of both time and collision number, and we determine the exponents related to these averages. In Section IV analytical arguments to determine some exponents and to derive a relation between the exponents of time and collision number analyses are discussed. Finally, we draw the conclusions in Section V, where we also present a summary of this present work.

## II. THE FERMI-ULAM MODEL

The Fermi-Ulam model describes the motion of a classical particle bouncing between two rigid walls, one of which is fixed at position  $x = 0$  and other that is moving periodically in time whose position is given by  $x_w(t'') = x_0 + \varepsilon' \cos(\omega t'' + \phi_0)$ . Here  $x_0$  is the equilibrium position,  $\varepsilon'$  is the oscillation amplitude,  $\omega$  is a frequency,  $t''$  is time and  $\phi_0$  is the initial phase. In order to work with dimensionless variables we perform scale changes in length  $X_w = x_w/x_0$  and in time  $t' = \omega t''$ . With these new variables the system has just one parameter, namely  $\varepsilon = \varepsilon'/x_0$ , and we write the position of the moving wall as  $X_w(t') = 1 + \varepsilon \cos(t' + \phi_0)$ . The particle moves freely between the walls and collides elastically with them. In this manner the FUM can be described by a map  $T(V_n, \phi_n) = (V_{n+1}, \phi_{n+1})$  which gives the velocity of the particle and the phase of the moving wall immediately after each collision [18]

$$T = \begin{cases} V_{n+1} = \pm V_n + 2\varepsilon \sin(\phi_{n+1}) \\ \phi_{n+1} = \phi_n + \Delta t_{n+1} \pmod{2\pi} \end{cases} \quad (1)$$

Here the term  $2\varepsilon \sin(\phi_{n+1})$  gives the fraction of velocity gained or lost in collision and  $\Delta t_{n+1} = t_{n+1} - t_n$  is the

time between two collisions with the moving wall, which is given by the smallest solution of

$$V_n \Delta t_{n+1} - (1 + \varepsilon \cos \phi_n) = \pm [1 + \varepsilon \cos(\Delta t_{n+1} + \phi_n)]. \quad (2)$$

The plus sign in the above equations corresponds to the situation in which the particle collides with the fixed wall before hitting the moving one (*indirect collisions*); the minus sign corresponds to the situation in which the particle hits successively with the moving wall (*direct collisions* or *successive collisions*).

Let us define  $V^2(t')$  as the square velocity at time  $t'$ . We are interested in the scaling properties of the dimensionless energy  $E = 2 \text{ Energy}/m\omega^2 x_0^2$  averaged over an ensemble of  $M$  samples that belong to the chaotic sea. Such samples are characterized by initial phases  $\phi_0$  of the moving wall randomly chosen in an interval  $I$ . If the initial velocity  $V_0$  is small enough then we can use  $I = [0, 2\pi)$ . Moreover we consider that the particle starts at the fixed wall position with velocity  $V_0 > 0$ . Thus, the time of the first collision of the particle with the moving wall is given by  $T_1 \approx 1/V_0$  and we define a variable  $t$  as  $t = t' - 1/V_0$ . In this way the time  $t$  starts at the first collision instant and we write the average energy as

$$E(t, \varepsilon, V_0) = \frac{1}{M} \sum_{j=1}^M V_j^2(t) \quad , \quad (3)$$

where  $j$  refers to a sample.

We consider also another kind of average where the square velocity is firstly averaged over the orbit of a sample as

$$\overline{V^2}(t') = \frac{1}{t'} \int_0^{t'} V^2(\tau) d\tau \quad , \quad (4)$$

and then we perform the average of the energy in an ensemble of  $M$  samples as defined below

$$\overline{E}(t, \varepsilon, V_0) = \frac{1}{M} \sum_{j=1}^M \overline{V_j^2}(t) \quad . \quad (5)$$

As the particle moves freely between the walls, the square of its velocity is constant between two impacts with the moving wall and the integral in Eq. (4) can be numerically evaluated without difficulties.

We will now describe some numerical procedures used to evaluate the averages quantities on time. The dynamics of FUM as described in Eq. (1) evolves in a discrete variable, namely the collision number  $n$ . As we are interested in the evolution of the average energies as defined in Eqs. (3) and (5), where time  $t$  is a continuous variable, we can use the map given by Eq. (1) to speed up the calculation process. We evaluate the averages in Eqs. (3) and (5) at discrete, logarithmic spaced, values of time  $t = t_1, t_2, \dots, t_N$ . We know that at  $t = 0$ , the first collision instant, the energy of the particle is  $V_1^2$  and, as the particle is at the moving wall position, the next collision takes place at  $t_c = \Delta t_2$ , where  $\Delta t_2$  is obtained by

solving Eq. (2). To evaluate the energy  $E_1$  of the first sample of the ensemble at time  $t = t_1$  we follow the procedure: (1) If  $t_1 \leq t_c$ , the energy of the particle at  $t_1$  will be  $E_1 = V_1^2$ . (2) Otherwise  $t_1 > t_c$  and a collision occurs at time  $t = t_c = \Delta t_2$ . Then we employ Eq. (1) updating the velocity of the particle to  $V_2$  and the next collision time is given by  $t_c = \Delta t_2 + \Delta t_3$ .

It means that if case 1 is satisfied then  $E_1(t_1)$  was determined. Otherwise we update the next collision instant and the velocity of the particle. If now  $t_1 \leq t_c$  (case 1) then  $E_1 = V_1^2$  but if  $t_1$  is still larger than  $t_c$ , we repeat case 2 updating both  $V$  and  $t_c$ . The reasoning is basically to repeat the above procedure until  $t_1 \leq t_c$  and then to update the energy  $E_1(t_1)$ . We follow a similar proceeding, with appropriate time intervals, to evaluate  $E_1(t_2)$ ,  $E_1(t_3)$ , ...,  $E_1(t_N)$ .

The procedure is the same for all samples of the ensemble giving  $E_2, \dots, E_M$  from  $t_1$  until  $t_N$ . Then the average energy in Eq. (3) is performed doing  $E(t_1) = [E_1(t_1) + E_2(t_1) + \dots + E_M(t_1)]/M$ , ...,  $E(t_N) = [E_1(t_N) + E_2(t_N) + \dots + E_M(t_N)]/M$ . The average energy  $\bar{E}(t, \varepsilon, V_0)$  in Eq. (5) can be evaluated by a similar procedure.

Since the map in Eq. (1) gives the velocity and phase after each collision with the moving wall, then the averages on variable  $n$  can be defined in a more direct manner. We first consider the average velocity over the orbit generated from an initial phase  $\phi_0$ , defined as  $\bar{V}^2(n) = \frac{1}{n+1} \sum_{i=0}^n V_i^2$ . Considering an ensemble with  $M$  samples, characterized by initial conditions that belong to the chaotic sea, we define the average energy as

$$\langle E \rangle (n, \varepsilon, V_0) = \frac{1}{M} \sum_{j=1}^M \bar{V}_j^2(n) . \quad (6)$$

### III. RESULTS

In Fig. 1(a) and 1(b) we show, respectively, the numerical results for the average energy  $E(t, \varepsilon, V_0)$  when the initial velocity is small, or  $V_0 \ll \varepsilon$ , and the situation in which  $V_0 \gg \varepsilon$ . The averages defined in Eqs. (3) and (5) were performed in an ensemble with  $M = 2 \times 10^3$  samples. Although  $V_0 \gg \varepsilon$ , the energy curves shown in 1(b) are obtained from orbits that belong to the chaotic sea. In Fig. 1(b) we used the same values of  $\varepsilon$  as those shown in Fig. 1(a).

As we can see more clearly in Fig. 1(a) the energy is constant until a time  $t_1$ , grows up to a time  $t_2$  and then reaches a stationary value for large values of time. As show in [20] the energy in the simplified FUM presents a slow decay in time. Since in SFUM the oscillating wall is considered fixed at position  $x = 1$ , the time between two collisions with the oscillating wall is  $2/V_n$ , and successive collisions do not occur. Therefore, if after a collision the particle has very low velocity, then it remains for a long time,  $2/V_n$ , with low energy. In this way, at time  $t$  many realizations are in such condition originating the

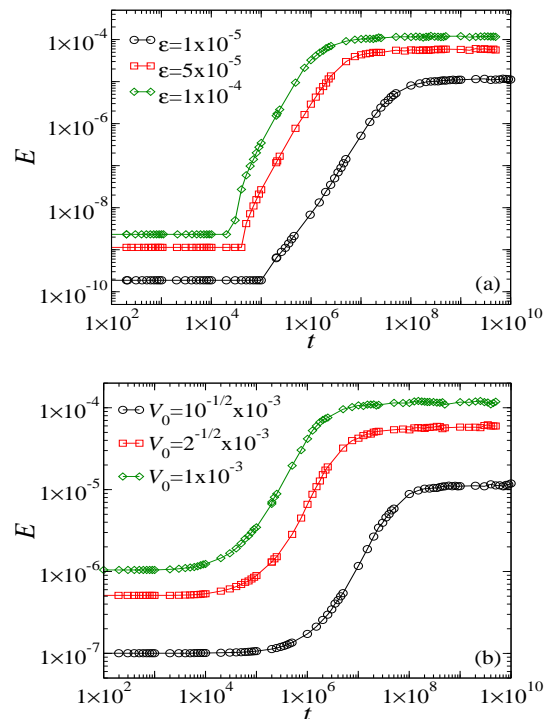


FIG. 1: (Color online) Log-log plots of the energy  $E(t)$  defined in Eq. (3), averaged over  $M = 2 \times 10^3$  samples, as function of time for (a) three values of  $\varepsilon$  and  $V_0 = 1 \times 10^{-6}$  ( $V_0 \ll \varepsilon$ ) and (b) three values of  $\varepsilon$ , the same ones as those shown in (a), and three values of initial velocity  $V_0 \gg \varepsilon$ .

slow decay in the average energy for  $t \gg t_2$ . In FUM this situation does not occur. If the particle, after a collision, losses almost all its energy, a successive collision occurs increasing the energy of the particle. Therefore, in FUM the average energy does not decay, but presents a saturation regime for  $t \gg t_2$ . Moreover, the energy for  $t \gg t_2$  can be described as

$$\begin{aligned} E(t, \varepsilon, V_0) &\propto g(\varepsilon) , \\ g(\varepsilon) &\propto \varepsilon^\beta . \end{aligned} \quad (7)$$

The value of exponent  $\beta$  can be determined by searching for the best collapse of the energy curves in the asymptotic regime. We performed simulations for values of  $\varepsilon$  between  $1 \times 10^{-5}$  and  $1 \times 10^{-3}$  and we obtained the average value  $\beta = 1.01 \pm 0.01$ . The crossover time  $t_2$  obeys the relation

$$t_2 \propto \varepsilon^z , \quad (8)$$

and the better fit in a plot of  $t_2$  as a function of  $\varepsilon$  gives  $z = -1.50 \pm 0.03$ , as shown in Fig. 2.

The time  $t_1$  is an average time in which the second indirect collisions happen. After that new collisions occur and the energy  $E(t, \varepsilon, V_0)$  begins to increase. Moreover,  $t_1$  is related to an initial transient and it affects the behavior of  $E(t, \varepsilon, V_0)$  for  $t \ll t_2$ . Therefore, between  $t_1$

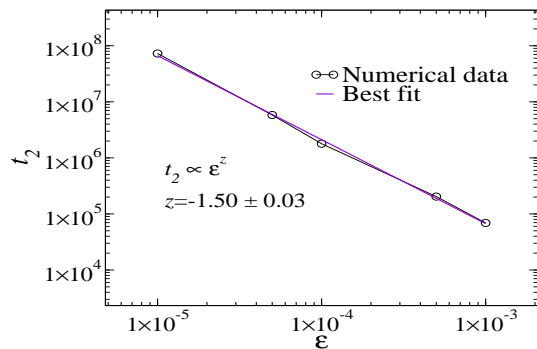


FIG. 2: Log-log plot of the crossover time  $t_2$  as function of parameter  $\varepsilon$ .

and  $t_2$  we have a crossover region in which the growth exponent can not be directly evaluated.

For large values of time ( $t \gg t_1$ ), the energy  $E(t, \varepsilon, V_0)$  can be written as a scaling function, namely

$$E(t, \varepsilon, V_0) = lE(l^a t, l^b \varepsilon, l^c V_0) . \quad (9)$$

Here  $a$ ,  $b$  and  $c$  are scaling exponents and  $l$  is the scaling factor. In the limit  $V_0 \ll \varepsilon$  (Fig. 1(a)) we can choose  $l = \varepsilon^{-1/b}$  and write the above equation as  $E(t, \varepsilon, 0) = \varepsilon^{-1/b} E(\varepsilon^{-a/b} t, 1, 0) \propto \varepsilon^{-1/b} f(\varepsilon^{-a/b} t)$ . For  $t \gg t_2$  this relation can be written as  $E(t, \varepsilon, 0) \propto \varepsilon^{-1/b}$ . Then, from Eq. (7) we have that  $\beta = -1/b$ . Using the simulation value  $\beta = 1.01 \pm 0.01$  we obtain  $b = -0.99 \pm 0.01$ . From Eq. (8) we derive the relation  $z = a/b$ . Since the simulations furnish  $z = -1.50 \pm 0.03$ , it follows that  $a = 1.49 \pm 0.04$ .

Fig. 3(a) shows the rescaled energy  $E(t, \varepsilon, V_0)/l$  as function of rescaled time  $tl^a$ . We can see that with these new coordinates the energy curves, originally depicted in Fig. 1(a), collapse onto a universal curve in the limit of long time, after an initial transient. We emphasize that the scaling behavior is valid only for small values of  $\varepsilon$ .

The argument to obtain the  $c$  exponent, namely  $c = b/2$ , is presented in the next section. Using this relation we obtain that  $c = -0.495 \pm 0.005$ . Fig. 3(b) shows the collapse of the curves depicted in Fig. 1(b) for the appropriate chosen initial velocities.

Depending on initial velocity and phase, the velocity after a collision with the moving wall can be very small in such way that a direct collision occurs and gives an immediate increase in energy. This scenario is more common for small values of  $V_0$  and  $t$  and does not allow us to find a scaling description to the initial transient at small values of  $t$ . However, this transient is important because it affects the power-law growth of the energy between  $t_1$  and  $t_2$ .

We can use Eqs. (7) and (8) to describe the average energy  $\bar{E}(t, \varepsilon, V_0)$ , defined in Eq. (5), as a scaling function just changing  $E$  by  $\bar{E}$ . Figs. 4(a) and 4(b) present the energy  $\bar{E}(t, \varepsilon, V_0)$  as function of time  $t$  for  $V_0 \ll \varepsilon$  (small initial velocity) and  $V_0 \gg \varepsilon$ , respectively. The values of  $\varepsilon$  are the same as those in Fig. 1(a). In Figs. 5(a)

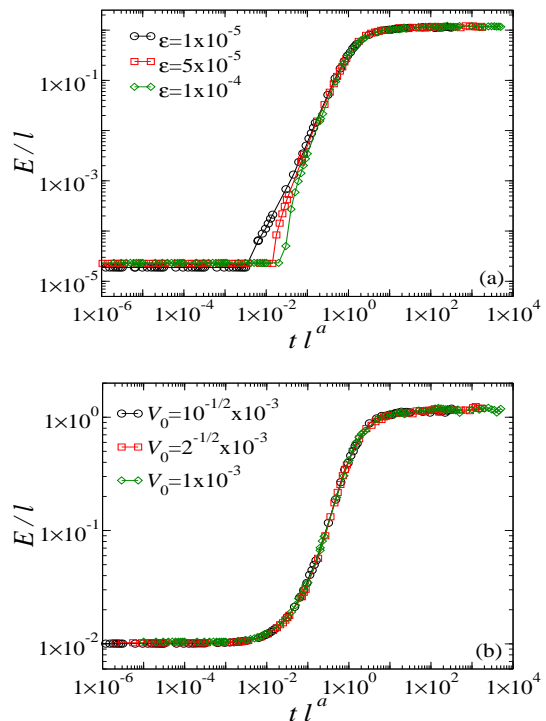


FIG. 3: (Color online) The rescaled energy  $E(t)/l$  as function of rescaled time  $tl^a$  for three values of  $\varepsilon$  in limit of long time. In (a) it is shown the collapse for  $V_0 \ll \varepsilon$  ( $V_0 = 1 \times 10^{-6}$ ) and in (b) the collapse for three values of initial velocity  $V_0 \gg \varepsilon$ . We chose  $l = \varepsilon^{-1/b}$  and the exponents are  $a = 1.49 \pm 0.04$ ,  $b = -0.99 \pm 0.01$  and  $c = -0.495 \pm 0.005$ .

and 5(b) it is shown the rescaled energy as function of rescaled time in limit of large  $t$  ( $t \gg t_1$ ). Following the same reasoning employed in analysis of the average energy  $E(t, \varepsilon, V_0)$ , we obtain the exponents  $a = 1.50 \pm 0.04$ ,  $b = -0.995 \pm 0.003$  and  $c = -0.498 \pm 0.001$ . Considering the uncertainties we observe that both averages  $E(t, \varepsilon, V_0)$  and  $\bar{E}(t, \varepsilon, V_0)$  are described by scaling functions with basically the same exponents set. Therefore, we will now use the average exponents  $a = 1.50 \pm 0.04$ ,  $b = -0.993 \pm 0.007$  and  $c = -0.497 \pm 0.003$ . Note that these values are different than the ones of the SFUM [20], namely,  $a_2 = 1.35 \pm 0.05$ ,  $b_2 = -0.90 \pm 0.03$  and  $c_2 = -0.45 \pm 0.01$ .

Fig. 6(a) shows the average energy  $\langle E \rangle(n, \varepsilon, V_0)$  for two values of  $\varepsilon$  and different initial velocities, including the situations (i)  $V_0 \ll \varepsilon$  and (ii)  $V_0 \gg \varepsilon$ . Now we have that

$$\langle E \rangle(n, \varepsilon, V_0) = l \langle E \rangle(l^{a^*} n, l^{b^*} \varepsilon, l^{c^*} V_0) . \quad (10)$$

We can determine the exponents  $a^*$  and  $b^*$  from the energy curves for  $V_0 \ll \varepsilon$ . When  $V_0 = 1 \times 10^{-6}$ , we observe in Fig. 6(a) that the average energy  $\langle E \rangle(n, \varepsilon, V_0)$  presents two regimes. For  $n < n_x$  the energy has a power-law growth and for  $n \gg n_x$  the energy is constant. Moreover, we obtain that  $n_x \propto \varepsilon^z$  with  $z = -1.01 \pm 0.02$ .

Since in the limit of large  $n$  the energy depends only

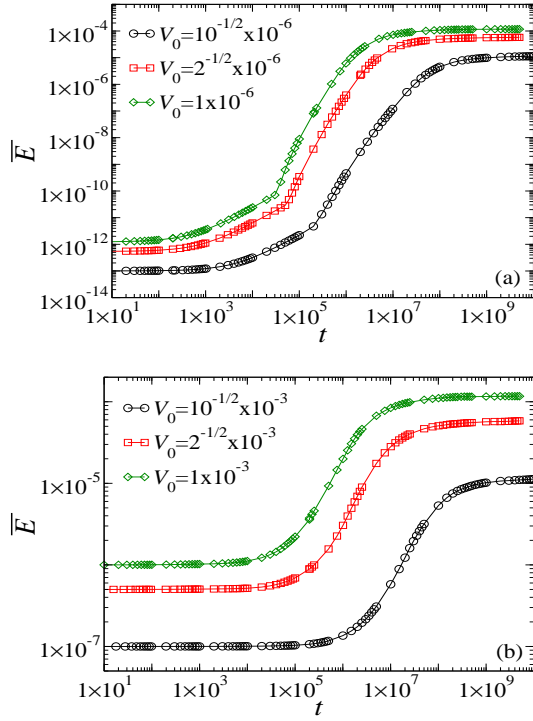


FIG. 4: (Color online) The average energy  $\overline{E}(t)$ , defined in Eq. (5), as function of time  $t$  for three values of  $\varepsilon$  and (a) three values of initial velocity  $V_0 \ll \varepsilon$  and (b) three values of velocity  $V_0 \gg \varepsilon$ . The averages were performed with  $M = 2 \times 10^3$  samples.

on  $\varepsilon$ , we have that  $\langle E \rangle(n, \varepsilon, V_0) = g(\varepsilon) \propto \varepsilon^\beta$  with  $\beta = 1.02 \pm 0.02$ . We can choose  $l = \varepsilon^{-1/b^*}$  and rewrite the above equation as  $\langle E \rangle(n, \varepsilon, V_0) = \varepsilon^{-1/b^*} \langle E \rangle(\varepsilon^{-a^*/b^*} n, 1, \varepsilon^{-c^*/b^*} V_0)$ . From this relation we obtain that  $z = a^*/b^* = -1.01 \pm 0.02$ . In limit  $n \gg n_x$  we can write  $\langle E \rangle(n, \varepsilon, V_0) \propto \varepsilon^{-1/b^*}$ . Therefore, we have that  $\beta = -1/b^* = 1.02 \pm 0.02$ . This implies that  $b^* = -0.98 \pm 0.02$  and  $a^* = 0.99 \pm 0.04$ . We use a connection between the simplified FUM and the standard map, described in the next section, to obtain the value of the exponent  $c^*$ , namely,  $c^* = b^*/2 = -0.49 \pm 0.01$ .

When  $V_0 \gg \varepsilon$  we observe in Fig. 6(a) that the energy curves present two characteristic iteration numbers,  $n'_x$  and  $n''_x$ . We can also observe that  $n''_x \approx 0$  for  $V_0 \ll \varepsilon$ . Therefore, we must consider two situations:  $n''_x \ll n'_x$ , for small initial velocities ( $V_0 \ll \varepsilon$ ), and  $n''_x \sim n'_x$ , for  $V_0 \gg \varepsilon$ . The energy curves with  $V_0 = 1 \times 10^{-6}$  ( $n''_x \approx 0$ ) present only two regimes: (1) a power-law growth for  $n \ll n'_x$  and (2) a saturation regime for  $n \gg n'_x$ . On the other hand, for the energy curves with  $V_0 = 1 \times 10^{-3}$  and  $V_0 = 10^{1/2} \times 10^{-3}$  ( $n''_x < n'_x$ ) shown in Fig. 6(a), we have three regimes: (1) the energy is basically constant for  $n \ll n''_x$ , (2) for  $n''_x < n < n'_x$  the energy grows and begins to follow the curve of  $V_0 = 1 \times 10^{-6}$  and (3) the energy curves reach a saturation regime for  $n \gg n'_x$ .

In Fig. 6(b) it is shown the rescaled energy  $\langle E \rangle / l$  as function of the rescaled interactions number  $nl^{a^*}$ . As

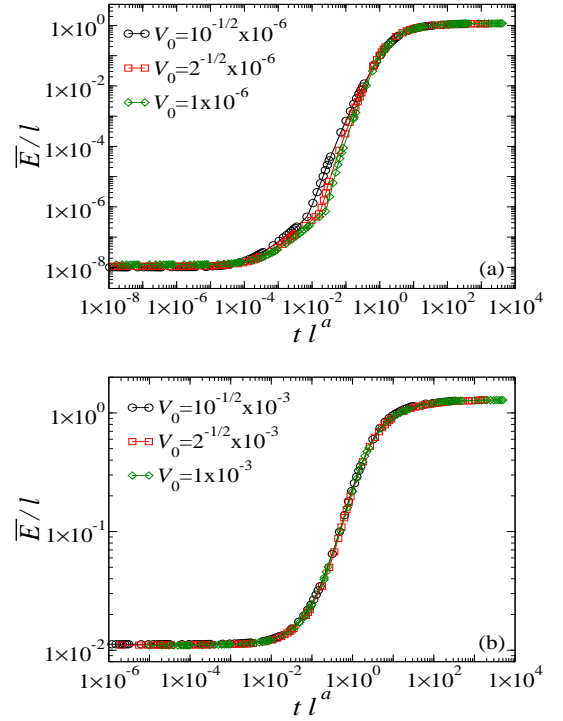


FIG. 5: (Color online) Log-log plots of the rescaled energy  $\overline{E}(t)/l$  as function of rescaled time  $tl^a$  in limit of large time for three values of  $\varepsilon$ . We have that (a)  $V_0 \ll \varepsilon$  and (b)  $V_0 \gg \varepsilon$ . We chose  $l = \varepsilon^{-1/b}$  and the exponents are  $a = 1.50 \pm 0.04$ ,  $b = -0.995 \pm 0.003$  and  $c = -0.498 \pm 0.001$ .

TABLE I: Numerical estimations of the scaling exponents for both FUM and SFUM. The exponents  $a$ ,  $b$  and  $c$  describe the scaling properties of the average energy as function of time  $t$  while the scaling relations of the average energy as function of collision number  $n$  are characterized by the exponents  $a^*$ ,  $b^*$  and  $c^*$ . The uncertainties are given between parenthesis.

	FUM		SFUM	
	$t$	$n$	$t$ [20]	$n$ [19]
$a, a^*$	1.50(4)	0.99(4)	1.35(5)	0.99(3)
$b, b^*$	-0.993(7)	-0.98(2)	-0.90(3)	-0.977(6)
$c, c^*$	-0.497(3)	-0.49(1)	-0.45(1)	-0.489(3)

we can observe, the energy curves, after a small initial transient, collapse onto a universal curve, even for  $V_0 \gg \varepsilon$ , with the exponents  $a^* = 0.99 \pm 0.04$ ,  $b^* = -0.98 \pm 0.02$  and  $c^* = -0.49 \pm 0.01$ . It is important to note that this set of exponents is the same, within the uncertainties, to that of the SFUM [19]. The exponents of the average energies as function of both time  $t$  and collision number  $n$  for the FUM and its simplification are shown in Table I.



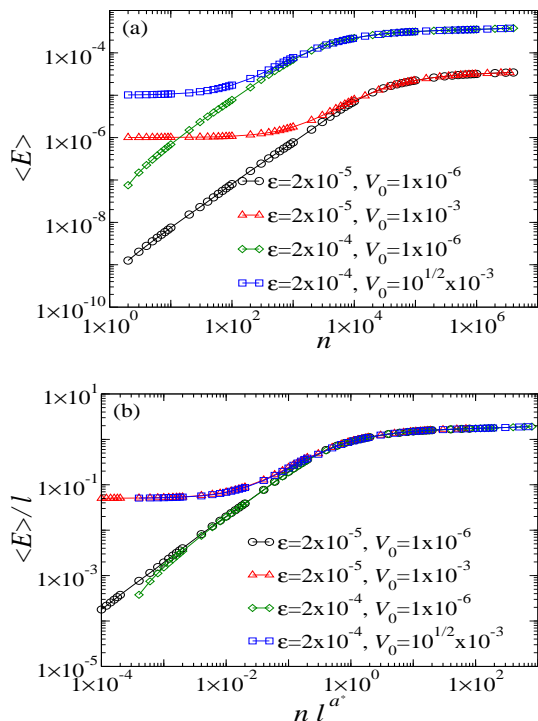


FIG. 6: (Color online) (a) Average energy for two values of  $\varepsilon$  and three values of initial velocity,  $V_0$ , as function of collision number,  $n$ . (b) The rescaled average energy as function of rescaled collision number shows that, after an initial transient, the energy curves collapse onto a universal curve.

#### IV. ANALYTICAL ARGUMENTS

Let us first derive a relation between the exponents  $c$  ( $c^*$ ) and  $b$  ( $b^*$ ). We follow the same lines of Leonel et al. [18]. Performing the variable change  $I_n = 2/V^* + 2(V^* - V_n/V^{*2})$ , where  $V^*$  is a typical velocity near to the lowest spanning curve, and a linearization around  $V^*$ , the FUM transforms into a standard map which is described by  $I_{n+1} = I_n - K_{\text{eff}} \sin \phi_{n+1}$  and  $\phi_{n+1} = \phi_n + I_n$ . Here  $K_{\text{eff}}$  is an effective control parameter given by  $K_{\text{eff}} = 4\varepsilon/V^{*2}$ . Note that the Standard model presents a transition from local to globally stochastic behavior at  $K = K_c \approx 0.972$ . The values of  $V^*$  in the lowest spanning curve of the FUM furnish a  $K_{\text{eff}}$  with value approximately the same as  $K_c$ , independent of  $\varepsilon$ . Then, we use the scaled variables  $\varepsilon' = l^b \varepsilon$  and  $V^{*'} = l^c V^*$  to obtain  $K_{\text{eff}} = 4\varepsilon'/V^{*'}{}^2 = 4(l^b \varepsilon)/(l^c V^*)^2$ . This implies that  $c = b/2$ .

Now we present an heuristic argument to support that  $c^* = -1/2$ . From Eq. (1) we can write, for  $n = 1$ , that

$$V_1^2 = V_0^2 \pm 4\varepsilon V_0 \sin(\phi_1) + 4\varepsilon^2 \sin^2(\phi_1). \quad (11)$$

A similar equation can be obtained for  $V_2^2$  by changing  $V_0$  by  $V_1$  and  $\phi_1$  by  $\phi_2$ . Then, we replace  $V_1^2$  by Eq. (11). This iteration procedure can be done for  $V_n^2$  with arbitrary  $n$ . If now we take the average in the ensemble of initial phases  $\langle V_n^2 \rangle$ , we always find a sum of three kinds of terms: (i)  $V_0^2$ , (ii) a set of terms  $\pm V_0 \varepsilon \langle \sin(\phi_j) \rangle$

and (iii) a set of terms  $\pm \varepsilon^2 \langle \sin(\phi_i) \sin(\phi_j) \rangle$ . Observe that  $\langle \sin(\phi_j) \rangle$  and  $\langle \sin(\phi_i) \sin(\phi_j) \rangle$  take values in the interval  $[-1, 1]$ . Since we are in the region below the first spanning curve, the maximal initial value  $V_{0,\text{max}}$  must be of order of  $V^* \approx \varepsilon^{1/2}$ . Therefore, for small  $\varepsilon$ ,  $V_0 \approx V_{0,\text{max}} \gg \varepsilon$  and  $n$  small enough we have that  $V_0^2 \lesssim \langle V_n^2 \rangle \gtrsim V_0^2$ , implying that  $\langle V_n^2 \rangle \approx V_0^2$ . Assuming that the scaling relation is valid in this limit, we obtain the relation  $\langle V_n^2 \rangle \approx l^{1+2c^*} \langle V_n^2 \rangle$ , which furnishes  $c^* = -1/2$ . It is worth mentioning that the numerical results for  $V_0 \gg \varepsilon$  shows that the scaling occurs in the beginning of the simulation without any transient (see Fig. (6)). Moreover, using the result  $c^* = b^*/2$ , we also obtain that  $b^* = -1$ .

Finally we present an argument that relates the exponents  $a^*$  and  $a$ , the scaling dimensions of variables  $n$  and  $t$ , respectively. As the average energy presents a saturation regime at large values of time, we can define the average velocity  $\bar{V} = \sqrt{\bar{E}}$  and  $\Delta t$  as the average time between two arbitrary collisions. We can also define  $\bar{L}$  as the average distance that the particle travels between these collisions in such way that we can write  $\bar{V} \Delta t / \bar{L} = \Delta n$ , where  $\Delta n$  is the average collisions number with the moving wall that take place in the time interval  $\Delta t$ . In terms of the rescaled variables we have that  $\bar{V}' \Delta t' / \bar{L}' = \Delta n'$ , or  $l^c \bar{V} l^a \Delta t / \bar{L} = l^{a^*} \Delta n$ . As  $\bar{L}' = \bar{L}$  we have, therefore, that the exponent of collision number,  $a^*$ , is related to the exponent of time,  $a$ , by  $a^* = a + c$ . This result is in good agreement with the simulations.

#### V. CONCLUSIONS

We studied the scaling properties of the chaotic sea below the lowest energy spanning curve of FUM considering average energies as function of time  $t$  and collision number  $n$ . In limit of large  $t$  ( $t \gg t_1$ ), the average energies  $E$  and  $\bar{E}$  of FUM can be described by scaling functions with exponents  $a \approx 3/2$ ,  $b \approx -1$  and  $c \approx -1/2$  (see Table I). This values are different than the ones of the SFUM [20], namely,  $a_2 = 1.35 \pm 0.05$ ,  $b_2 = -0.90 \pm 0.03$  and  $c_2 = -0.45 \pm 0.01$ . The scaling descriptions of the average energies are also hold on variable  $n$ , with exponents  $a^* \approx 1$ ,  $b^* \approx -1$  and  $c^* \approx -1/2$ . These values are basically the same as those of the SFUM [19]. We employed some analytical arguments to determine the exponents  $c^* = -1/2$  and  $b^* = -1$ . We observe also that, in the full model, the scaling exponents related to variables  $\varepsilon$  and  $V_0$  are, within the uncertainties, the same for both  $n$  and  $t$  analyses, or  $b^* \approx b$  and  $c^* \approx c$ . We can also note that the exponents related to the variables  $t$  and  $n$  ( $a$  and  $a^*$ , respectively) are note the same. However, we provide an heuristic argument that establishes a connection between these exponents by the relation  $a^* = a + c$ . It is important to stress that the scaling analysis only holds for small values of the rescaled amplitude  $\varepsilon$ , close enough to the integrable ( $\varepsilon = 0$ ) to non-integrable ( $\varepsilon \neq 0$ ) transition. Moreover, we observe that the energy of the FUM

is constant up to a time  $t_1$ , grows to a time  $t_2$  and, then, reaches a stationary value. In the SFUM the average energy, differently of FUM, presents a slow decay for large  $t$  ( $t \gg t_2$ ) [20]. This striking result is a consequence of the approximation used to define the SFUM. As the oscillating wall is considered fixed in space, the time between collisions is  $2/V$  and successive collisions do not occur. Therefore, eventually after a collision with the moving wall, the particle has very low velocity  $V$  and remains for a long time ( $2/V$ ) with low energy, originating a slow decay in energy for  $t \gg t_2$ . In the full model it is different: if after a collision with the moving wall the particle losses almost all its energy, then a successive collision occurs increasing the energy of the particle and the decay in energy at  $t \gg t_2$  is not observed. The analyses on variable  $n$  furnish basically the same results for both FUM and SFUM because between one arbitrary collision and the next one we always have that  $\Delta n = 1$ , independently if the collisions are direct (successive) or indirect.

Summarizing, we employed scaling analyses to describe the properties of average energies as function of  $t$  and as function of  $n$  in regime of small amplitudes of oscillation of the moving wall,  $\varepsilon \approx 0$ , for the full Fermi-Ulam model. We observe that i) the scaling exponents related to the variables  $\varepsilon$  and  $V_0$  are basically the same for both  $t$  and  $n$  analyses, namely,  $b \approx b^* \approx -1$  and  $c \approx c^* \approx -1/2$ . ii)

We also observe that the scaling exponents related to the variables  $t$  and  $n$  are not the same,  $a \approx 3/2$  and  $a^* \approx 1$ , respectively, and, by a simple analytical reasoning, we show that these exponents are connected by the relation  $a^* = a + c$ . iii) Performing some analytical analyses on variable  $n$  we derive that  $b^* = -1$  and  $c^* = -1/2$ . iv) Considering also the results of the simplified Fermi-Ulam model, [19] and [20], we observe that the scaling analyses of FUM and SFUM on variable  $t$  are characterized by different exponents sets, while the analyses on variable  $n$  furnish, basically, the same exponents set for both FUM and SFUM. v) We observe also that the successive collisions play an important rule when the Fermi-Ulam model is studied on variable  $t$  by, mainly, preventing the energy decay for long times. vi) In the analysis on variable  $n$  direct (successive) and indirect collisions play a similar rule and, therefore, the energy curves as function of  $n$  present, for both FUM and SFUM, the same behavior and they are described by a single set of scaling exponents.

We thank to J.A. Plascak for the careful reading of the manuscript. D.G.L. and J.K.L.S. were partially supported by Conselho Nacional de Pesquisa (CNPq). J.K.L.S. also thanks to Fundação de Amparo à Pesquisa do Estado de Minas Gerais (FAPEMIG).

\* Electronic address: dgl@fisica.ufmg.br

† Electronic address: jaff@fisica.ufmg.br

- 
- [1] E. Fermi, Phys. Rev. **15**, 1169 (1949).  
 [2] A. J. Lichtenberg and M.A. Lieberman, *Regular and Chaotic Dynamics* (Appl. Math. Sci. **38**, Springer Verlag, New York, 1992).  
 [3] M.A. Lieberman and A. J. Lichtenberg, Phys. Rev. A **5**, 1852 (1971).  
 [4] R. Douady (1982), *Applications du théorème des tores invariants*, Thèse de 3ème Cycle, Univ. Paris VII.  
 [5] L. D. Pustil'nikov, Trudy Moskov. Mat. Obsc. **34** (2), 1 (1977), L. D. Pustil'nikov, Theor. Math. Phys. **57**, 1035 (1983); L. D. Pustil'nikov, Sov. Math. Dokl. **35**(1), 88 (1987); L. D. Pustil'nikov, Russ. Acad. Sci. Sb. Math. **82**(1), 231 (1995).  
 [6] A. J. Lichtenberg, M.A. Lieberman and R. H. Cohen, Physica D **1**, 291 (1980).  
 [7] E. D. Leonel and P. V. E. McClintock, J. Phys. A **38**, 823 (2005).  
 [8] E. D. Leonel and P. V. E. McClintock, J. Phys. A **38**, L425 (2005).  
 [9] G. Karner, J. Stat. Phys. **77**, 867 (1994).  
 [10] S. T. Dembinski, A. J. Makowski and P. Peplowski, Phys. Rev. Lett. **70**, 1093 (1993).  
 [11] J. V. José and R. Cordery, Phys. Rev. Lett. **56**, 290 (1986).  
 [12] Z. J. Kowalik, M. Franaszek and P. Pieranski, Phys. Rev. A **37**, 4016 (1988).  
 [13] S. Warr, W. Cooke, R. C. Ball and J. M. Huntley, Physica A **231**, 551 (1996).  
 [14] N. Saitô, H. Hirooka, J. Ford, F. Vivaldi and G. H. Walker, Physica D **5**, 273 (1982).  
 [15] E. Canale, R. Markarian, S. O. Kamphorst and S. P. de Carvalho, Physica D **115**, 189 (1998).  
 [16] A. Loskutov, A. B. Ryabov and L. G. Akinshin, J. Phys. A: Math. Gen. **33**, 7973 (2000).  
 [17] A. Loskutov and A. B. Ryabov, J. Stat. Phys. **108**, 995 (2002).  
 [18] E. D. Leonel, J. K. L. da Silva and S. O. Kamphorst, Physica A **331**, 435 (2004).  
 [19] E. D. Leonel, P. V. E. McClintock and J. K. L. da Silva, Phys. Rev. Lett. **93**, 14101 (2004).  
 [20] D. G. Ladeira and J. K. L. da Silva Phys. Rev. E **73**, 026201 (2006).